Original Research

Regional heterogeneity in rat Peyer's patches through whole transcriptome analysis

Charles L Phillips[1,2], Bradley A Welch[2], Michael R Garrett[3] and Bernadette E Grayson[2]

[1]Program in Pathology, University of Mississippi Medical Center, Jackson, MS 39216, USA; [2]Department of Neurobiology and Anatomical Sciences, University of Mississippi Medical Center, Jackson, MS 39216, USA; [3]Department of Pharmacology, University of Mississippi Medical Center, Jackson, MS 39216, USA

Corresponding author: Bernadette E Grayson. Email: bgrayson@umc.edu

Impact statement

Peyer's patches are gut-associated lymphoid tissue dispersed throughout the intestine. Their role is to guard the organism from orally ingested invaders. Likewise, they can permit modulation of the immune system through gut entry. Here, through transcriptomics, we compare the proximally located PP to more distally located PP and observe a significant level of non-overlap between the PP derived from unique segments. These data will help understand the complex role the PP play in gut immune health.

Abstract

Peyer's patches are gut-associated lymphoid tissue located throughout the intestinal wall. Peyer's patches consist of highly organized ovoid-shaped follicles, classified as non-encapsulated lymphatic tissues, populated with B cells, T cells, macrophages, and dendritic cells and function as an organism's intestinal surveillance. Limited work compares the gene profiles of Peyer's patches derived from different intestinal regions. In the current study, we first performed whole transcriptome analysis using RNAseq to compare duodenal and ileal Peyer's patches obtained from the small intestine of Long Evans rats. Of the 12,300 genes that were highly expressed, 18.5% were significantly different between the duodenum and ileum. Using samples obtained from additional subjects ($n = 10$), we validated the novel gene expression patterns in Peyer's patches obtained from the three regions of the small intestine. Rats had a significantly reduced number of Peyer's patches in the duodenum in comparison to either the jejunum or ileum. Regional differences in structural, metabolic, and immune-related genes were validated. Genes such as alcohol dehydrogenase 1, gap junction protein beta 2, and serine peptidase inhibitor clade b, member 1a were significantly reduced in the ileum in comparison to other regions. On the other hand, genes such as complement C3d receptor type, lymphocyte cytosolic protein 1, and lysozyme C2 precursor were significantly lower in the duodenum. In summary, the gene expression pattern of Peyer's patches is influenced by intestinal location and may contribute to its role in that segment.

Keywords: Peyer's patches, immune system, rat model, barrier function

Experimental Biology and Medicine **2021; 246: 513–522. DOI: 10.1177/1535370220973014**

Introduction

Gut-associated lymphoid tissue (GALT) consists of organized lymphoid structures lining the gastrointestinal tract that contains both isolated and aggregated multifollicular structures for protection or prevention of invading pathogenic organisms from ingested material.[1] Peyer's patches (PP) are specialized ovoid-shaped GALT classified as non-encapsulated lymphatic tissue and are predominantly found in the distal jejunum and ileum but are also more recently described in the duodenum.[2,3] PP primarily function as immune sentinels of the small intestine. PP's specific role is to monitor bacterial populations and protect against pathogenic bacteria in the intestine, in addition to maintaining tolerance to commensal bacteria and food.

PP are estimated to contain over 70% of the body's immune cells.[3] The population of cells within PP, e.g., microfold cells, macrophages, dendritic cells, B-lymphocytes, and T-lymphocytes, allow PP to uptake and trap foreign particles, survey luminal contents, and destroy pathogenic microorganisms.[3] Thus, PP significantly influence immunity and various immune-related diseases. For example, PP are necessary for the establishment of oral tolerance to ingested proteins[3] and allergic sensitization to food components.[4] On the other hand, the activity of the PP contributes substantially to the lack of effectiveness in oral vaccines versus parenterally administered vaccines.[5,6] Beyond that, pathogenic gastrointestinal infections alter the migration and induction of immune cells via the PP.[7,8]

Though PP were first described in the ileum,[2] PP can be identified in the jejunum and the duodenum.[9] The majority of the focus of study has been on PP within the ileum. However, given that proximally located PP have primary exposure to orally ingested food stuffs, drug therapies, and other ingestible substances, understanding the molecular differences between the proximal and distally located PP is essential to investigate.

This work aimed to compare the gene profiles of PP obtained from the three segments of the small intestine. First, we performed whole transcriptome analysis using RNAseq to understand the regional differences between the proximally identified duodenal patches with more distally located ileal patches. We then used additional samples to validate the findings using jejunal-derived PP to add further regional context. Taken as a whole, regional differences in gene expression of structural and immune-related genes may help us further understand the complexity of their contribution to gut immunity.

Materials and methods

Animal assurance

All procedures for animal use complied with the Guidelines for the Care and Use of Laboratory Animals by the National Research Council of the National Academies. Procedures were reviewed and approved by the University of Mississippi Medical Center Institutional Animal Care and Use Committee (IACUC #1423). In conducting research using animals, the investigators adhered to the laws of the United States of America and regulations of the Department of Agriculture.

Animals

Male Long Evans rats (~450 g/18 weeks old, $n = 10$) purchased from Envigo (Indianapolis, IN) were singly housed in the University of Mississippi Medical Center under controlled conditions (12:12 light-dark cycle, 50–60% humidity, 25°C) with free access to water.

Euthanasia

Animals were 6 h fasted and then euthanized. The intestine was externalized, and PP counted in each region of the intestine and carefully dissected and stored in PFA or frozen for RNA/protein extraction.

Peyer's patch quantification

After the externalization of the small intestine, PP were counted by measured segment (10 cm duodenum, ~40 cm jejunum, and ~60 cm ileum). Each of the segments were partitioned based on the measurements previously listed and the first PP from each segment was used thereby assuring similar placement of the PP with respect to the intestinal segment between animals.

Tissue histology

Peyer's patches from rat small intestine were collected and fixed with PFA and paraffin-embedded at room temperature. Samples were sectioned at 5 μm and mounted on slides. The hematoxylin and eosin-stained sections were then imaged with an Olympus BX60 microscope at 10×. Slides were also submitted to the UMMC Pathology Department for digital scanning (PHILIPS Digital Pathology Solutions Image Management System, Philips, Netherlands) and lengths of PP obtained.

RNA processing

Peyer's patches were visualized externally and microdissected and immediately frozen on dry ice then stored at −80°C until further processing. RNA was isolated with TRIzol® and extracted using a QIAGEN miniprep RNA kit (QIAGEN, Inc., Valencia, CA). RNA content was quantified using the NanoDrop Lite (Fisher ThermoScientific, Waltham, MA). All samples displayed a purity level of greater than 2.0.

Whole transcriptome analysis

The samples submitted to the Genomics Core for RNAseq analysis for RNAseq were banked duodenal and ileal PP samples of male Long Evans rats (500 g, $n = 3$). These samples were processed for RNAseq by the UMMC Genomics Core. Briefly, RNA was assessed for quality control parameters of minimum concentration and fidelity (i.e. 18S and 28S bands, RQI >8). Libraries were developed using the TruSeq mRNA Stranded Library Prep Kit (Set-A-indexes), quantified with the Qubit fluorimeter (Invitrogen), and assessed for quality and size using Bio-Rad Experion System. Samples were pooled into a single library ($n = 10$ pooled samples per library) and sequenced using the NextSeq 500 High Output Kit (300 cycles, paired-end 100 bp) on the Illumina NextSeq 500 platform. The run generated 124 Gb at QC30 = 85.6% with 605 million or 60 million reads per sample passing filter. Sequenced reads were assessed for quality using the Illumina BaseSpace Cloud Computing Platform, and FASTQ sequence files were used to align reads to the rat reference genome using RNA-Seq Alignment Application (using STAR aligner). On average, 58 million reads (or >94% reads per sample) mapped to the reference genome per sample. Differential expression was determined using Cufflinks Assembly & DE workflow (v2.1.0) or DESeq2. Gene expression differences are denoted as Log2 (ratio) and $q > 0.05$.

Gene networks and functional analysis were evaluated using Ingenuity Pathways Analysis (IPA, Ingenuity® Systems, www.ingenuity.com). Canonical pathways were identified using gene data comparing the duodenal to ileal PP with P values greater than 0.20. The IPA figure displays entities that have a –log (P-value) greater than 5.0.

Taqman real-time PCR

Total RNA was used to transcribe to complementary DNA using an iScript complementary DNA synthesis kit (Bio-Rad Laboratories, Hercules, CA). Quantitative polymerase

chain reaction was performed on a Step-One Plus Real-Time PCR machine coupled with StepOne Software (v2.3) (Applied Biosystems) using TaqMan inventoried gene expression assays (Life Technologies, Foster City, CA). Samples were analyzed in duplicate, and changes in Ct values from the internal control 60 s ribosomal protein 32 (RPL32) were calculated. The control group average ΔCt was made to equal 1. ΔCts of the control group and the experimental groups were then compared, and the fold change was calculated, creating a 2ΔΔCt paradigm. Data were then multiplied by 100 so that the control group average ΔCt equaled 100.

Statistical analyses

All statistical analyses were performed using GraphPad Prism version 8.0 (GraphPad Software, San Diego, California, USA). One-way ANOVA with repeated measures was used to observe regional differences of the paired samples and Tukey's test for regional *post hoc* analysis. All results are given as means ± SEM. Results were considered statistically significant when $P < 0.05$.

Results

Whole transcriptome analysis

Sequencing of the rat intestinal PP assessed 12,300 of the 17,327 annotated genes. The Illumina software-generated comparisons of the normalized mean count versus the $\log^2$ fold change. Of the 12,300 genes probed, 10,021 were not different between the duodenal PP and ileal PP (Figure 1(a), insignificant in green), whereas 2279 genes or 18.5% were differentially expressed (Figure 1(a), significant in red) between duodenal PP and ileal PP. The Illumina software generated a heat map to visualize the strength of differences between the differentially expressed genes, where high expression values are labeled in green and low expression in red (Figure 1(b)). The top 25 genes with the greatest differential expression and their expression counts are listed in Table 1.

Using two lists of differential expression sequencing counts for duodenum and ileum set *post hoc* at ≥300, we visualized the depth of overlap between the two regions using a Venn diagram (Figure 1(c)). Of the 7769 duodenal genes and 8393 ileal genes with counts ≥300, 7600 or 88.8% overlapped (Figure 1(c)); 168 genes or 2% of the genes were unique to the duodenum (Figure 1(c)); 792 genes or 9.3% were unique to the ileum (Figure 1(c)). The most highly expressed duodenal genes by count are presented (Table 2a) along with the list of the most-highly expressed ileal genes (Table 2b). Fifteen of the genes in this abbreviated list overlap (Table 2), underscoring that the most highly expressed genes in the duodenum and the most highly expressed genes in the ileum are expressed in common. Further, IPA's canonical pathway analysis of duodenal PP and ileal PP showed both up- (depicted in red) and down- (depicted in green) regulation of pathways involved in cell turnover, immune signaling, and metabolism (Figure 1(d)).

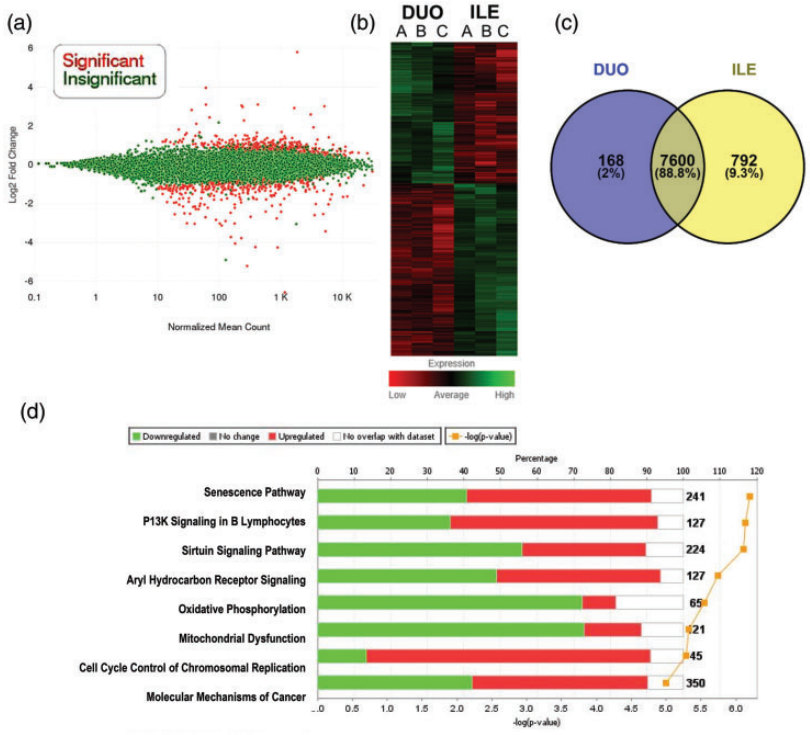

Figure 1. RNAseq data for duodenal PP and ileal PP of CH animals. (a) MA plot of genes compared depicting those with significant differences (2279 in red) and insignificant differences (10,021 in green). (b) Heat map representing genes of duodenal PP and ileal PP clustered based on expression values, higher expression in green and lower expression in red. (c) Venn diagram illustrating the relationship between highly expressed genes of duodenal PP and ileal PP. (d) Canonical pathway analysis of duodenal and ileal PP, upregulated genes shown in red and downregulated genes shown in green. Pathways overall relate to cell cycle process, immune signaling, and energy metabolism.

Table 1. Genes with a significant difference in expression in duodenal PP and ileal PP.

		Duodenal PP			Ileal PP			
SYMBOL	Gene name	Mean		SEM	Mean		SEM	*P* value
Tlr9	Toll-like receptor 9	347.67	±	12.41	551.67	±	2.73	0.00009
Ccni	Cyclin I	4236.33	±	194.35	7384.00	±	53.00	0.00010
Chsy1	Chondroitin sulfate synthase 1	754.00	±	38.08	1385.33	±	29.49	0.00020
Aldh4a1	Aldehyde dehydrogenase 4 family member A1	430.00	±	27.79	902.67	±	26.41	0.00025
Clcn4	Chloride voltage-gated channel 4	667.33	±	41.03	1270.00	±	35.79	0.00038
Cr2	Complement C3d receptor 2	9091.33	±	629.74	18787.67	±	926.00	0.00098
Tmem150a	Transmembrane protein 150 A	711.67	±	37.49	325.00	±	25.15	0.00102
Adh1	Alcohol dehydrogenase 1 A	9175.67	±	591.77	1583.00	±	699.46	0.00116
Ppm1k	Protein phosphatase, Mg2+/Mn2+ Dependent 1 K	649.00	±	32.81	1486.67	±	95.96	0.00117
Serpinb6	Serpin family B member 6	8743.00	±	565.76	3137.33	±	385.70	0.00121
Gjb2	Gap junction protein beta 2	5766.33	±	620.53	559.67	±	296.74	0.00163
Msn	Moesin	6286.67	±	444.50	11830.67	±	591.68	0.00170
Riok3	RIO kinase 3	3323.00	±	188.22	5356.33	±	199.69	0.00177
Pdk2	Pyruvate dehydrogenase kinase 2	649.67	±	20.08	355.33	±	34.69	0.00183
Atox1	Antioxidant 1 copper chaperone	1890.00	±	79.07	1232.67	±	42.29	0.00184
Nin	Ninein	642.00	±	37.45	1775.33	±	152.33	0.00195
Uvrag	UV radiation resistance-associated gene protein	637.00	±	53.53	1244.67	±	66.85	0.00208
Hdac9	Histone deacetylase 9	328.67	±	14.38	768.33	±	61.38	0.00222
Mtpn	Myotrophin	1679.33	±	33.93	3947.67	±	325.51	0.00227
Chst3	Carbohydrate sulfotransferase 3	320.00	±	27.54	517.33	±	7.31	0.00228
Actg1	Actin, gamma 1	7713.67	±	184.84	12527.67	±	685.90	0.00247
Cybb	Cytochrome B-245 beta chain	1549.00	±	14.73	3488.00	±	286.55	0.00250
Cd5l	CD5 molecule like	980.67	±	267.60	2970.33	±	124.28	0.00252
Serpinb1a	Serpin family B member 1	13981.00	±	915.94	5169.00	±	937.14	0.00255
Ccng2	Cyclin G2	2844.00	±	250.08	4600.33	±	77.37	0.00257

PP distribution

Total number of visible PP in rats ranged from as few as 14 to as many as 22 (Figure 2(a)). The number of PP significantly differed based on the region of the small intestine with the least amount of PP present in the duodenum, $P < 0.0001$ (Figure 2(a)). Using the Philips Digital Software for measurement of the length of each PP in the intestinal wall, the PP of the ileum were substantially greater in length than either the duodenum or jejunum, $P < 0.05$ (Figure 2(b)). PP were not examined for other histologic changes in this study. Representative images of PP by relative intestinal location show PP tissue morphology (Figure 2(c)). No gross differences were observed morphologically by region outside of overall palpable size.

Gene expression changes by region

The RNAseq data were validated using genes of interest that were expressed more highly in the duodenal PP than ileal PP. Alcohol dehydrogenase 1 (ADH1) gene expression varied significantly, $P < 0.01$, with a lower expression in ileal PP in comparison to both duodenal and jejunal PP by *post hoc* analysis (Figure 3(a)). Gap junction protein beta 2 (GJB2) gene expression also varied significantly by region, $P < 0.001$, with significantly lower expression in ileal PP in comparison to both duodenal and jejunal PP (Figure 3(b)). Serine peptidase inhibitor clade b, member 1a (SERPINB1A) expression varied significantly by region, $P < 0.01$, with ileal expression lower than jejunal (Figure 3(c)) and serine peptidase inhibitor clade b, member 1 b (SERPINB1B) gene expression varied by region, $P < 0.001$, with expression significantly lower in the ileal PP in comparison to duodenal and jejunal PP (Figure 3(d)).

We next validated genes that were significantly reduced in the duodenum in comparison to the ileum by RNAseq analysis. Actin gamma 1 (ACTG1) expression varied significantly by region, $P < 0.01$, with lower expression in the duodenal PP in comparison to jejunal PP (Figure 3(e)). Complement C3d receptor type 2 (CR2), associated with mature B cells, had significantly different expression based on PP location within the intestine, $P < 0.01$, and duodenal PP expression was significantly lower than both jejunal and ileal PP by *post hoc* analysis (Figure 3(f)). Lymphocyte cytosolic protein 1 (LCP1) expression varied significantly by PP location in the intestine, $P < 0.05$ and duodenal PP had lower LCP1 expression than either jejunal or ileal PP (Figure 3(g)).

Expression for lysozyme C2 precursor (LYZ2), a lysozyme encoding gene, differed significantly by intestinal region in PP, $P < 0.001$ (Figure 3(h)). Duodenal expression is significantly lower than both jejunal and ileal PP; further, jejunal PP expression is significantly lower than ileal (Figure 3(h)). Moesin (MSN), membrane-organizing extension spike protein, expression significantly varied by region, $P < 0.001$ with duodenal expression being significantly lower than jejunal (Figure 3(i)).

Immune target genes in PP

Gene expression of cluster of differentiation 3 (CD3), CD68, integrin alpha X (ITGAX), specific to leukocytes and highly

Table 2. Genes that are highly expressed in duodenal PP and genes that are highly expressed in ileal PP.

Symbol	Gene name	Mean		SEM
a. Highly expressed duodenual genes				
Cd74	CD74 molecule, MHC, class II invariant chain	53257.7	±	6003.3
Eef1a1	Eukaryotic translation elongation factor 1 alpha 1	41736.3	±	1768.8
Eef2	Eukaryotic translation elongation factor 2	36360.7	±	2130.7
Srrm2	Serine/arginine repetitive matrix 2	29874.7	±	2023.4
Clu	Clusterin	28810.0	±	3680.6
Fth1	Ferritin heavy chain 1	26361.7	±	2991.4
Myh11	Myosin heavy chain 11	25714.3	±	8627.4
Hsp90ab1	Heat shock protein 90 alpha family class B member 1	23869.3	±	1657.2
Tpt1	Tumor protein, translationally-controlled 1	23678.0	±	1250.1
RT1-Da	Major histocompatibility complex, class II, DR alpha	23454.7	±	2124.2
Macf1	Microtubule actin crosslinking factor 1	23100.7	±	1049.0
B2m	Beta-2-microglobulin	22065.7	±	1105.8
Tmsb4x	Thymosin beta 4 X-linked	21673.3	±	1515.5
Ptprc	Protein tyrosine phosphatase receptor type C	20706.3	±	1032.2
Atp5b	ATP synthase F1 subunit beta	19412.7	±	1521.9
Mfge8	Milk fat globule-EGF factor 8 protein	18908.7	±	2118.3
RT1-Ba	Major histocompatibility complex, class II, DQ alpha 1	18273.7	±	1843.7
Ddx5	DEAD (Asp-Glu-Ala-Asp) box helicase 5	18260.0	±	407.6
b. Highly expressed ileal genes				
Cd74	CD74 molecule, MHC, class II invariant chain	59837.3	±	2662.6
Eef2	Eukaryotic translation elongation factor 2	59410.3	±	3752.7
Eef1a1	Eukaryotic translation elongation factor 1 alpha 1	55100.7	±	2624.6
Hsp90ab1	Heat shock protein 90 alpha family class B member 1	36334.0	±	1238.6
Lcp1	Lymphocyte cytosolic protein 1	35712.3	±	3713.7
Ptprc	Protein tyrosine phosphatase receptor type C	34493.3	±	2498.5
Srrm2	Serine/arginine repetitive matrix 2	31538.0	±	3542.2
Clu	Clusterin	30823.3	±	2695.7
B2m	Beta-2-microglobulin	29402.0	±	1815.4
RT1-Da	Major histocompatibility complex, class II, DR alpha	28784.3	±	1914.8
Tpt1	Tumor protein, translationally controlled 1	28609.0	±	1302.6
Tmsb4x	Thymosin beta 4 X-linked	27021.7	±	1916.8
Mfge8	Milk fat globule-EGF factor 8 protein	26623.0	±	3202.7
Pabpc1	Poly(A) binding protein cytoplasmic 1	26540.7	±	2383.0
Lyz2	Lysozyme	25915.7	±	1588.7
Macf1	Microtubule actin crosslinking factor 1	25202.7	±	2611.2
Coro1a	Coronin 1 A	23518.3	±	2954.1
RT1-Ba	Major histocompatibility complex, class II, DQ alpha 1	23279.3	±	1511.0
Ddx5	DEAD (Asp-Glu-Ala-Asp) box helicase 5	22913.3	±	1790.4

expressed by dendritic cells, and transforming growth factor beta (TGFβ) did not significantly differ by region (Figure 4(a), (d), (f), and (i)). T cell-associated genes, CD4 and CD8, expression were different by intestinal region of PP, $P < 0.05$ and $P < 0.001$, respectively (Figure 4(b) and (c)). CD4 jejunal expression was significantly higher than ileal expression and jejunal expression of CD8 was significantly higher than both duodenal and ileal expression, $P < 0.01$ (Figure 4(b) and (c)). Protein tyrosine phosphatase receptor, type C (PTPRC), expression varied significantly, $P < 0.001$, with jejunal expression being significantly higher than either duodenal or ileal expression, $P < 0.05$ (Figure 4(e)). Additionally, lipopolysaccharide binding protein (LBP) expression was elevated in the jejunum, $P < 0.05$ (Figure 4(g)). The gene expression of interleukin 1 beta (IL1β), a cytokine that signals macrophage activation, significantly varied by region, $P < 0.01$, with both duodenal and ileal expression significantly lower than jejunal expression, $P < 0.01$ and $P < 0.05$, respectively (Figure 4(h)).

Discussion

Our work demonstrates the significant difference in duodenal numbers of PP versus the number of PP in either the jejunum or ileum. The disparity in the number of PP by region is congruent with human studies that show a reduced number of PP in the duodenum in comparison to PP in either the jejunum or ileum.[2,10] Measurements of individual PP length were significantly different, with the largest PP observed in the ileum. This characteristic is reported in earlier human studies that also state that PP from the ileum are larger than those of other regions of the small intestine.[2]

The expression profile of the small intestine is known to vary by segmental location and is influenced by the role of that segment. For example, cytochrome b reductase 1 integral in metabolism of iron is expressed only in the duodenum.[11] In contrast, lactase-phlorizin hydrolase (*Lct*) is mainly expressed in the jejunum,[12] and the apical sodium-dependent bile acid

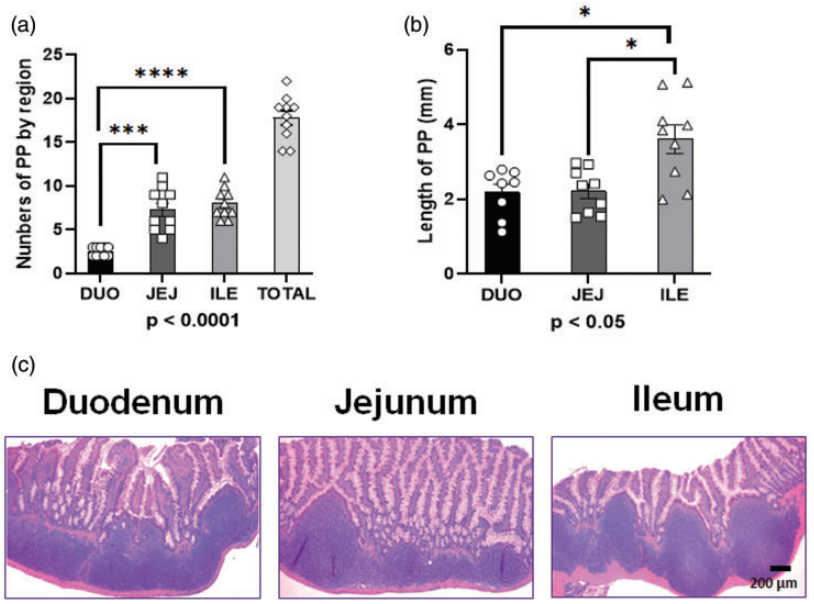

Figure 2. PP by intestinal region. (a) PP number by region of the intestine compared to overall total PP. (b) Measurements of length of the PP by region. (c) Representative images of hematoxylin and eosin (H&E) at 10× magnification. Data are presented as mean ± SEM and analyzed by one-way ANOVA. *$P < 0.05$, **$P < 0.01$, ****$P < 0.0001$.

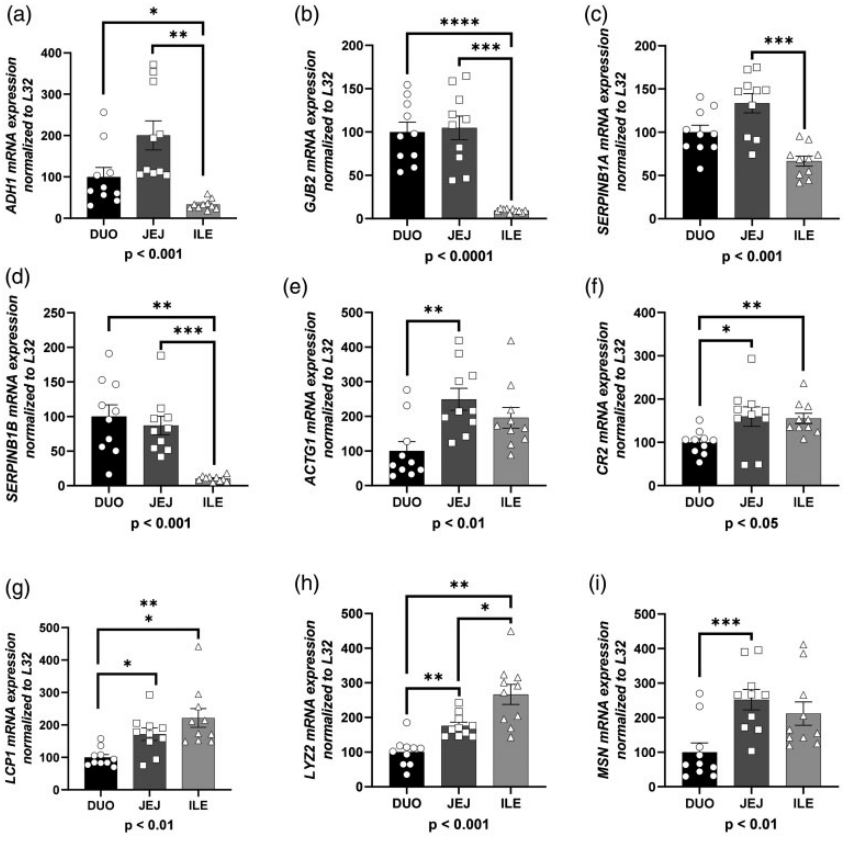

Figure 3. Gene expression of target validation of the RNAseq in PP from duodenum, jejunum, and ileum. (a) Alcohol dehydrogenase 1 (ADH1) (b) Gap junction protein beta 2 (GJB2) (c) Serine peptidase inhibitor clade b, member 1a (SERPINB1A) (d) serine peptidase inhibitor clade b, member 1 b (SERPINB1B) (e) Actin gamma 1 (ACTG1) (f) Complement C3d receptor type 2 (CR2) (g) Lymphocyte cytosolic protein 1, (LCP1) (h) Lysozyme C2 precursor (i) Moesin (MSN). Data are presented as mean ± SEM. Statistical comparison of region and diet performed by one-way ANOVA reported below each graph with *post hoc* Tukey's. Relevant statistical comparison reported by *$P < 0.05$, ** $P < 0.01$, ***$P < 0.001$, ***$P < 0.0001$ ($n = 10$/group).

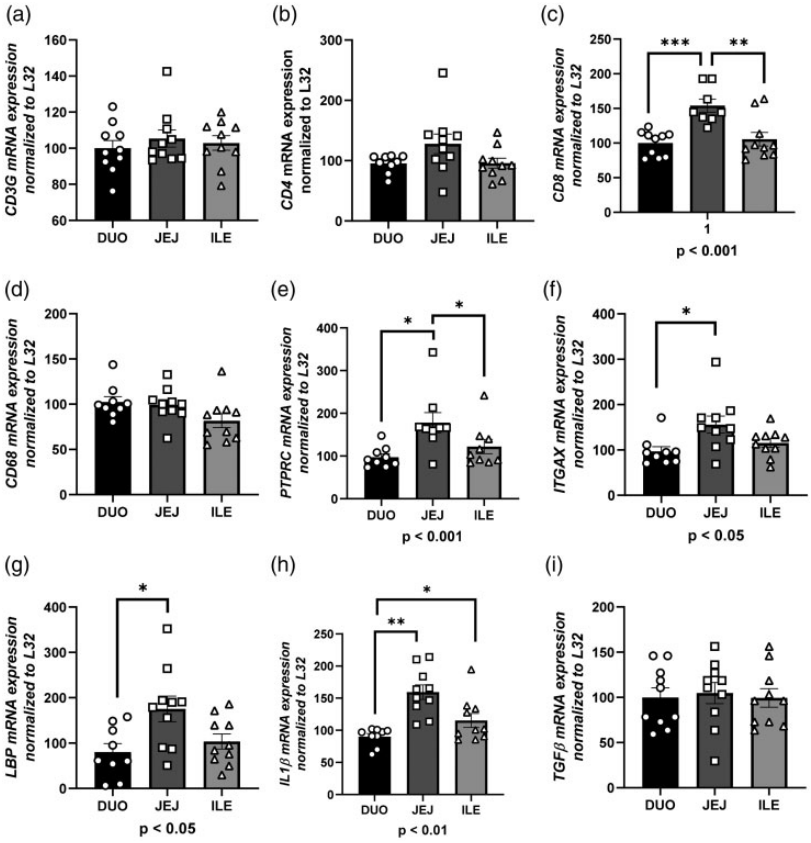

Figure 4. Gene expression analysis of immune targets in PP from duodenum, jejunum, and ileum (a) CD3 (b) CD4 (c) CD8 (d) CD68 (e) Protein tyrosine phosphatase receptor, type C (PTPRC) (f) Integrin alpha X (ITGAX) (g) Lipopolysaccharide binding protein (LBP) (h) Interleukin 1 beta (IL1β) (i) Transforming growth factor beta (TGFβ). Data are presented as mean ± SEM. Statistical comparison of region and diet performed by two-way ANOVA reported below each graph with *post hoc* Tukey's Relevant statistical comparison reported by $^*P < 0.05$ ($n = 10$/group).

transporter (ASBT, *Slc10a2*) most highly expressed in the ileum.[13]

Given that differences have been reported based on segment, our initial thoughts were that the most robust differences in gene expression would be obtained comparing the duodenal to the ileal PP. This assumption is the rationale behind choosing PP from these regions for the whole transcriptome analysis. We did find diverse roles of the PP in the various pathways identified by the analysis. For example, the senescence pathway is associated with cellular growth, proliferation, and development, and is a response to physiological or pathological stressors that leads to cell cycle arrest. In the gut, this pathway prevents the development of various gastrointestinal cancers.[14] In contrast, sirtuin signaling delays senescence and further prolongs cellular life expectancy.[15] Members of the sirtuin family have been connected to obesity and related comorbidities, and in recent literature, connected to inflammation.[16] P13K activation regulates actions in the development, activation, and differentiation of both B and T lymphocytes; additionally, P13K activation has both negative and positive responsibilities in immunity.[17] In B lymphocytes, P13K signaling regulates cell metabolism following activation, thus linking B cell metabolism with receptor signaling.[18] Aryl hydrocarbon receptor signaling is relevant to cell cycle regulation in that it acts as a cell cycle checkpoint, arresting cell cycle before DNA replication, outside of its responsibilities in drug metabolism.[19] Finally, the Cell Cycle Control of Chromosomal Regulation canonical pathway ensures that DNA replication occurs correctly in the cell cycle and is not occurring with damaged or stressed cells.[20] Taken together, pathways demonstrating variance between PP from different regions largely revolves around checks within the cell cycle.

Differential expression of genes by region in the intestine

The genes used to validate the RNAseq data generally fell into two categories: structural networking proteins or immune-modulating proteins. First, we validated gene targets that were more highly expressed in proximal PP in comparison to the distal PP of the gut followed by validating targets more highly expressed in distal PP.

The PP are predominantly made of resident immunocytes; the expression of ADH1 has previously been identified in tissues of myeloid and lymphoid origin and can trigger differentiation of M1 macrophages and induce production of IL-1β, IL-6, and TNF-α.[21] Further, the gastric epithelium is a primary site for the conversion of alcohol and aldehydes/ketones in humans and rodents.[22] The higher expression proximally may be a byproduct of proximity to the stomach and the need for detoxification due to location. Similarly, GJB2 expression, which encodes the

connexin 26 protein, is greater in proximal PP and is highly expressed in follicle-associated epithelium and microfold cells of PP.[23] Connexin proteins are abundant in the digestive system and primarily form gap junctions. Gap junctions formed by connexin 26 allow for the transport of ions and certain small molecules.[24] Certain pathogens exploit this junctional protein such as enteropathogenic *E. coli,* which can co-opt the expression of connexin 26 for gastrointestinal invasion and, ultimately, diarrhea.[25] Significantly higher expression of GJB2 in PP close to the stomach facilitates increased susceptibility to pathogens that would exploit this protein for infection. Furthermore, an upregulation in gap junction related proteins would be indicative of more gap junctions present, thus more channels to transport molecules and ions.

SERPINB1A/B, serine peptidase inhibitors of clade B, are also known as leukocyte elastase inhibitors. They are important in neutralizing protease activity and protecting tissues from inflammatory damage.[26] Higher expression SERPINB1A/B in the duodenum and jejunum could be due to these segments being more closely located to the stomach where the unprocessed nutrient load is high and where greater neutralization is necessary. Furthermore, SERPINB1A has been shown to be upregulated in the intestinal mucosa of mice with ulcerative colitis,[27] suggesting its role to compensate for the damage produced to the intestine in this disease process. Caspases mediate defense against microbial infections and produces pro-inflammatory cytokines that can trigger pyroptosis, inflammatory cell death with substantial cytosolic leakage.[28] Unchecked caspase activity could thus lead to a deleterious inflammatory process and requires regulation; SERPINB1 limits the activation of inflammatory caspases preventing their unsolicited activation.[28]

ACTG1 is a highly conserved structural protein of the cytoskeleton present in many tissues throughout the body and is highly expressed in the intestine, with higher levels in the distal intestine than the proximal intestine. Increased ACTG1 may signify a difference in the scaffolding that makes up the PP of the ileum given that the ileal PP are much larger in comparison to the duodenal PP. Considering ingested contents become more compact during transit within the small intestine as nutrients are absorbed, and waste is transported to the lower gastrointestinal tract,[29] there may be a greater need for higher structural integrity.

CR2 encodes for complement C3d receptor, an essential part of the complement system. CR2 is expressed on the surfaces of B cells and T cells[30] and follicular dendritic cells[31] and participates in their activation and maturation. CR2 protein by immunoelectron microscopy has been found on the cell surface of cells localized to the light zone of the germinal center in PP.[32] On the other hand, LCP1 encodes for plastin-2 and is an actin-binding protein that is expressed in the intestinal epithelium. Plastin in humans has two distinct isoforms. The L isoform is expressed only in hematopoietic cell lineages and the T isoform is found in solid tissues with replicative potential.[33] Moreover, LCP1 is an activator of T cells.[34] The high presence of CR2 and LCP1 in the distal gut may be protective against pathogens who have survived the extended distance to arrive in the ileum.

LYZ2 is an enzyme with bacteriolytic function and is active against a range of Gram-positive and -negative bacteria.[35] Given that the ileum is closest to the cecum where the largest concentration of microbiota resides, it is not entirely surprising that LYZ2 is highly expressed here. Further, PP contain unique subsets of lysozyme expressing cells, which fortify their antimicrobial roles.[36] Finally, MSN (moesin), also known as the membrane organizing extension protein, functions as a cross-linker between plasma membranes and actin cytoskeletons. Along with the proteins, ezrin, and radixin, moesin forms specialized membrane domains and apical microvilli of epithelial cells.[37] Similar to ACTG1, it may provide structural integrity to the PP under tension.

PP expression of immune-related genes

PP contain immune cells such as B cells, T cells, macrophages, and dendritic cells that are compartmentalized into three domains and are surrounded by a follicle-associated epithelium separating the cells of the PP from luminal content. The follicle-associated epithelium contains specialized microfold cells that allow the entrance of antigens and bacteria into the PP for processing by immune cells.[38] Surprisingly, there was higher expression patterns of T cell marker CD8, generalized markers for lymphocytes PTPRC, and the dendritic and macrophage cell marker ITGAX in the jejunal PP. There is higher expression of cytokine IL1β in the jejunum, aligning with immune cell marker expression. IL1β is secreted by leukocytes, such as macrophages, and is produced as the inactive pro-IL-1β precursor in response to pathogen-associated molecular patterns, which is then cleaved by caspase-1.[39] As the duodenum is very short in comparison to the jejunum, it may be that its contribution of immune health is more complicated than is currently known.

Limitations and future directions

In hindsight, whole transcriptome analysis of each region's representative PP would have been useful to expand our knowledge concerning PP rather than at the ends of the intestine. In the directed PCR we performed stemming from the RNAseq, we were surprised to find high expression of transcripts in the jejunum in comparison to either the duodenum or ileum. We surmise there may be an undescribed role of jejunal PP to be discovered. Rather than excising representative PP from each segment of the intestine, excising a representative PP for every given measure of length would showcase whether a gradient of expression exists in certain transcripts based on the function of that segment of the intestine. This procedure would require frequent sampling over the length of the intestine but may expand our understanding of the role of PP. The strength here is that we excised the first PP encountered after a standard length that was measured each time for each segment.

The PP are nestled amidst the surrounding epithelium of the gut. Some targets we probed may overlap with normal intestinal tissues; thus, it is possible that some of the tissue

included in each sampling in the current study is more properly intestinal tissue and not PP alone. More precise methods of tissue collection could overcome this heterogeneity, such as microscopy coupled with laser capture dissection. In the future, such a method might yield greater homogeneity of expression. Finally, given that the gut and microbiome housed within the gut make accommodations to the diet of the host, it would be interesting in the future to determine whether transcript regulation occurs as a result of the macronutrient content of the diet.

AUTHORS' CONTRIBUTIONS

All authors participated in the design, interpretation of the studies and analysis of the data and review of the manuscript; CLP, BAW, MRG, and BEG conducted the experiments, CLP, BAW, MRG, and BEG analyzed the data. CLP and BEG wrote the manuscript, CLP, BAW, MRG, and BEG edited and approved the final draft.

DECLARATION OF CONFLICTING INTERESTS

The author(s) declared no potential conflicts of interest with respect to the research, authorship, and/or publication of this article.

FUNDING

The work performed through the UMMC Molecular and Genomics Facility is supported, in part, by funds from the NIGMS, including Mississippi INBRE (P20GM103476), Obesity, Cardiorenal and Metabolic Diseases-COBRE (P20GM104357), and Mississippi Center of Excellence in Perinatal Research (MS-CEPR)-COBRE (P20GM121334). The content of the manuscript is solely the responsibility of the authors and does not necessarily represent the official views of the National Institutes of Health.

ORCID ID

Bernadette E Grayson https://orcid.org/0000-0002-1281-1682

REFERENCES

1. Donaldson DS, Else KJ, Mabbott NA. The gut-associated lymphoid tissues in the small intestine, not the large intestine, play a major role in oral prion disease pathogenesis. *J Virol* 2015;**89**:9532–47
2. Cornes JS. Number, size, and distribution of Peyer's patches in the human small intestine: part I the development of Peyer's patches. *Gut* 1965;**6**:225–9
3. Jung C, Hugot JP, Barreau F. Peyer's patches: the immune sensors of the intestine. *Int J Inflam* 2010;**2010**:823710
4. Roth-Walter F, Berin MC, Arnaboldi P, Escalante CR, Dahan S, Rauch J, Jensen-Jarolim E, Mayer L. Pasteurization of milk proteins promotes allergic sensitization by enhancing uptake through Peyer's patches. *Allergy* 2008;**63**:882–90
5. van der Lubben IM, Verhoef JC, van Aelst AC, Borchard G, Junginger HE. Chitosan microparticles for oral vaccination: preparation, characterization and preliminary in vivo uptake studies in murine Peyer's patches. *Biomaterials* 2001;**22**:687–94
6. Shakweh M, Ponchel G, Fattal E. Particle uptake by Peyer's patches: a pathway for drug and vaccine delivery. *Expert Opin Drug Deliv* 2004;**1**:141–63
7. Shreedhar VK, Kelsall BL, Neutra MR. Cholera toxin induces migration of dendritic cells from the subepithelial dome region to T- and B-Cell areas of Peyer's patches. *Infect Immun* 2003;**71**:504–9
8. Nagai S, Mimuro H, Yamada T, Baba Y, Moro K, Nochi T, Kiyono H, Suzuki T, Sasakawa C, Koyasu S. Role of Peyer's patches in the induction of Helicobacter pylori-induced gastritis. *Proc Natl Acad Sci U S A* 2007;**104**:8971–6
9. Van Kruiningen H, Ganley L, Freda B. The role of Peyer's patches in the age-related incidence of Crohn's disease. *J Clin Gastroenterol* 1997;**25**:470–5
10. Van Kruiningen HJ, West AB, Freda BJ, Holmes KA. Distribution of Peyer's patches in the distal ileum. *Inflamm Bowel Dis* 2002;**8**:180–5
11. McKie AT, Barrow D, Latunde-Dada GO, Rolfs A, Sager G, Mudaly E, Mudaly M, Richardson C, Barlow D, Bomford A, Peters TJ, Raja KB, Shirali S, Hediger MA, Farzaneh F, Simpson RJ. An iron-regulated ferric reductase associated with the absorption of dietary iron. *Science* 2001;**291**:1755–9
12. Krasinski SD, Upchurch BH, Irons SJ, June RM, Mishra K, Grand RJ, Verhave M. Rat lactase-phlorizin hydrolase/human growth hormone transgene is expressed on small intestinal villi in transgenic mice. *Gastroenterology* 1997;**113**:844–55
13. Shneider BL. Intestinal bile acid transport: biology, physiology, and pathophysiology. *J Pediatr Gastroenterol Nutr* 2001;**32**:407–17
14. Penfield JD, Anderson M, Lutzke L, Wang KK. The role of cellular senescence in the gastrointestinal mucosa. *Gut Liver* 2013;**7**:270–7
15. Lee SH, Lee JH, Lee HY, Min KJ. Sirtuin signaling in cellular senescence and aging. *BMB Rep* 2019;**52**:24–34
16. Zhou S, Tang X, Chen H-Z. Sirtuins and insulin resistance. *Front Endocrinol* 2018;**9**:748
17. So L, Fruman DA. PI3K signalling in B- and T-lymphocytes: new developments and therapeutic advances. *Biochem J* 2012;**442**:465–81
18. Jellusova J, Rickert RC. The PI3K pathway in B cell metabolism. *Crit Rev Biochem Mol Biol* 2016;**51**:359–78
19. Puga A, Xia Y, Elferink C. Role of the aryl hydrocarbon receptor in cell cycle regulation. *Chem Biol Interact* 2002;**141**:117–30
20. Sclafani RA, Holzen TM. Cell cycle regulation of DNA replication. *Annu Rev Genet* 2007;**41**:237–80
21. Liu Y, Ou Y, Sun L, Li W, Yang J, Zhang X, Hu Y. Alcohol dehydrogenase of Candida albicans triggers differentiation of THP-1 cells into macrophages. *J Adv Res* 2019;**18**:137–45
22. Haselbeck RJ, Duester G. Regional restriction of alcohol/retinol dehydrogenases along the mouse gastrointestinal epithelium. *Alcoholism Clin Exp Res* 1997;**21**:1484–90
23. Kobayashi A, Donaldson DS, Kanaya T, Fukuda S, Baillie JK, Freeman TC, Ohno H, Williams IR, Mabbott NA. Identification of novel genes selectively expressed in the Follicle-Associated epithelium from the Meta-Analysis of transcriptomics data from multiple mouse cell and tissue populations. *DNA Res* 2012;**19**:407–22
24. Maeda S, Nakagawa S, Suga M, Yamashita E, Oshima A, Fujiyoshi Y, Tsukihara T. Structure of the connexin 26 gap junction channel at 3.5 Å resolution. *Nature* 2009;**458**:597–602
25. Simpson C, Kelsell DP, Marchès O. Connexin 26 facilitates gastrointestinal bacterial infection in vitro. *Cell Tissue Res* 2013;**351**:107–16
26. Law RHP, Zhang Q, McGowan S, Buckle AM, Silverman GA, Wong W, Rosado CJ, Langendorf CG, Pike RN, Bird PI, Whisstock JC. An overview of the serpin superfamily. *Genome Biol* 2006;**7**:216
27. Naito Y, Takagi T, Okada H, Omatsu T, Mizushima K, Handa O, Kokura S, Ichikawa H, Fujiwake H, Yoshikawa T. Identification of inflammation-related proteins in a murine colitis model by 2D fluorescence difference gel electrophoresis and mass spectrometry. *J Gastroenterol Hepatol* 2010;**25(Suppl 1)**:S144–8
28. Choi YJ, Kim S, Choi Y, Nielsen TB, Yan J, Lu A, Ruan J, Lee H-R, Wu H, Spellberg B, Jung JU. SERPINB1-mediated checkpoint of inflammatory caspase activation. *Nat Immunol* 2019;**20**:276–87
29. Rendtorff ND, Zhu M, Fagerheim T, Antal TL, Jones M, Teslovich TM, Gillanders EM, Barmada M, Teig E, Trent JM, Friderici KH, Stephan DA, Tranebjærg L. A novel missense mutation in ACTG1 causes dominant deafness in a Norwegian DFNA20/26 family, but ACTG1

mutations are not frequent among families with hereditary hearing impairment. *Eur J Hum Genet* 2006;**14**:1097–105
30. Levy E, Ambrus J, Kahl L, Molina H, Tung K, Holers VM. T lymphocyte expression of complement receptor 2 (CR2/CD21): a role in adhesive cell-cell interactions and dysregulation in a patient with systemic lupus erythematosus (SLE). *Clin Exp Immunol* 1992;**90**:235–44
31. Liu Y-J, Xu J, de Bouteiller O, Parham CL, Grouard G, Djossou O, de Saint-Vis B, Lebecque S, Banchereau J, Moore KW. Follicular dendritic cells specifically express the long CR2/CD21 isoform. *J Exp Med* 1997;**185**:165–70
32. Yamakawa M, Imai Y. Complement activation in the follicular light zone of human lymphoid tissues. *Immunology* 1992;**76**:378–84
33. Lin C-S, Park T, Chen ZP, Leavitt J. Human plastin genes. Comparative gene structure, chromosome location, and differential expression in normal and neoplastic cells. *J Biol Chem* 1993;**268**:2781–92
34. Wabnitz GH, Kocher T, Lohneis P, Stober C, Konstandin MH, Funk B, Sester U, Wilm M, Klemke M, Samstag Y. Costimulation induced phosphorylation of L-plastin facilitates surface transport of the T cell activation molecules CD69 and CD25. *Eur J Immunol* 2007;**37**:649–62
35. Markart P, Faust N, Graf T, Na C-L, Weaver TE, Akinbi HT. Comparison of the microbicidal and muramidase activities of mouse lysozyme M and P. *Biochem J* 2004;**380**:385–92
36. Bonnardel J, Da Silva C, Henri S, Tamoutounour S, Chasson L, Montanana-Sanchis F, Gorvel JP, Lelouard H. Innate and adaptive immune functions of Peyer's patch monocyte-derived cells. *Cell Rep* 2015;**11**:770–84
37. Saotome I, Curto M, McClatchey AI. Ezrin is essential for epithelial organization and villus morphogenesis in the developing intestine. *Dev Cell* 2004;**6**:855–64
38. Jung C, Hugot J-P, Barreau F. Peyer's patches: the immune sensors of the intestine. *Int J Inflamm* 2010;**2010**:823710
39. Lopez-Castejon G, Brough D. Understanding the mechanism of IL-1β secretion. *Cytokine Growth Factor Rev* 2011;**22**:189–95

(Received July 23, 2020, Accepted October 20, 2020)